#### **PAPER • OPEN ACCESS**

# Combined wind turbine design and wind farm layout optimisation under wind resource uncertainty

To cite this article: S Krishna Swamy et al 2020 J. Phys.: Conf. Ser. 1618 042030

View the <u>article online</u> for updates and enhancements.



# IOP ebooks™

Bringing together innovative digital publishing with leading authors from the global scientific community.

Start exploring the collection-download the first chapter of every title for free.

**1618** (2020) 042030

doi:10.1088/1742-6596/1618/4/042030

# Combined wind turbine design and wind farm layout optimisation under wind resource uncertainty

S Krishna Swamy<sup>1</sup>, S Szklarz<sup>2</sup>, R M Fonseca<sup>2</sup> and B H Bulder<sup>1</sup>

TNO Energy Transition, 1755 LE Petten, The Netherlands TNO Energy Transition, 3584 CB Utrecht, The Netherlands

Email: siddharth.krishnaswamy@tno.nl

Abstract. Applications of the wind farm layout optimisation problem focus on optimally positioning a certain number of turbines within a wind farm so that annual energy production (AEP) is maximised. This study addresses an earlier stage in the wind farm development process. Instead of optimising the individual positions of a certain number of turbines of a selected model, the control variables in the optimisation are rotor diameter of a wind turbine of fixed nominal power, number of turbines in a wind farm of fixed area and orientation angle of turbines in the farm. In addition to AEP, this study considers capital and operational expenses of a wind farm to calculate the levelized cost of energy (LCoE), which is the objective function. Given the stage of development addressed, it is also essential that uncertainty is considered; here the focus is on the impact of wind resource uncertainty. The optimisation is performed with a recently developed state-of-the-art stochastic gradient based method (StoSAG) which has shown in different domains to be computationally efficient and accurate when dealing with optimisation problems under uncertainty. Our results show non-trivial optimal designs with LCoE reductions of ~0.5% compared to the most optimal solution from a sensitivity analysis.

#### 1. Introduction & Literature

The cumulative installed capacity of offshore wind power in the EU has increased from 622 megawatts (MW) in the year 2004 to 22,072 MW at the end of 2019, with over 3,600 MW added in 2019 [1]. With increasingly crowded offshore space in certain parts of the North and Baltic Seas, it is essential that optimisation for minimised Cost of Energy is considered from the earliest stages of development, even though the information available may have high uncertainty. The objective of this work is to perform a combined wind turbine design and wind farm layout optimisation to find the ideal type, number and orientation of turbines in an offshore wind farm. With the increasing visibility of atmospheric changes due to climate change, the design of wind farms and turbines should be performed by accounting for different types of uncertainties which impact energy generation in wind farms. In this work, uncertainty in wind resource is introduced from historical data at a reference site to achieve wind farm design under uncertainty i.e. find a more robust optimal design strategy.

The power production of a turbine can be increased by lengthening the blade, although longer blades lead to higher investment costs and reduced spacing between turbines in a given area. Similarly, placing too many turbines in a farm will increase production, but incur additional investment costs and higher wake effects. Given these trade-offs, finding the right rotor diameter and number of turbines in a given farm area is an optimisation problem, and a decision that needs to be made by wind farm developers.

Studies on wind turbine optimisation to find a trade-off between blade length and hub height have been performed using particle swarm optimisation [2] and differential evolution algorithm [3]. Gradient

Published under licence by IOP Publishing Ltd

Content from this work may be used under the terms of the Creative Commons Attribution 3.0 licence. Any further distribution of this work must maintain attribution to the author(s) and the title of the work, journal citation and DOI.

**1618** (2020) 042030

doi:10.1088/1742-6596/1618/4/042030

based optimisation of farms with different turbine heights has shown decrease in cost of energy by 5-9% [4]. Optimising the parameters and performance of fixed and variable speed wind turbines at a specific site condition has shown improvements in profitability and cost of energy [5].

A frequently attempted problem when optimising a wind farm is the wind farm layout optimisation problem (WFLOP), where individual turbine locations are optimised for, making the number of control variables (~100). Non-uniform wind farms (i.e. wind farms with multiple types of turbines and hubheights) were seen to achieve lower costs of energy compared to their regular counterparts, when using an extended random search algorithm [6]. Another study by the same authors solves the WFLOP for Horns Rev 1 considering inter-annual conditions of the wind resource to introduce robustness in the optimisation [7]. The layout of Horns Rev 1 wind farm is optimised for power production with a genetic algorithm and a choice between four commercial turbine types in [8].

Coupled wind turbine design and layout optimisation is explored in [9] and performs better than sequentially optimising single variables, although no uncertainty in wind resource is accounted for. Wind turbine type and placement optimisation is explored with genetic algorithms with Class I, II and III type turbines [10]. Combined optimisation of turbine characteristics (tower height and rotor diameter) and wind farm layout has been shown to reduce LCoE and increase AEP at a German site in [11]. Optimal turbine configurations tended to more conservative designs i.e. larger ratios of swept area to power produced when uncertainty was introduced in [12].

Among the sources of uncertainty in wind farm layout evaluation such as uncertainty in wind speed, wake modelling, thrust (Ct) curve, surface roughness, power curve, capital costs, annual O&M costs and discount rate, uncertainty in wind speed proved to be most sensitive to the resulting AEP [13], and is chosen in this study. A mathematical approach to account for uncertainty in wind resource assessment is discussed by Lackner et. al [14] and Kwon [15]. An analysis of wind resource uncertainty showed that bulk regression between monitoring and reference sites provide more accurate long term wind speed projections than directional regressions [16].

In reality, wind farm design optimisation is fraught with uncertainties since a potential location is modelled using uncertain data sources such as frequency of wind from various directions, Weibull distribution to define wind speeds etc. To achieve optimisation solutions which have practical value, it is imperative to account for uncertainty within the optimisation framework known as robust optimisation. One way of representing uncertainty is to generate multiple models (or an ensemble) which represent the system being modelled. Most optimisation methods are not suitable for robust optimisation due to their computational inefficiency. This study uses a recently developed state-of-the-art optimisation technique, Stochastic Simplex Approximate Gradient (StoSAG) introduced by Fonseca et. al (2017), to achieve robust optimisation of wind farm design.

Considering the literature discussed above, this study contributes in the following ways. For a combined wind turbine design and wind farm layout optimisation, rather than using a discrete set of wind turbine configurations, the design space is fully explored to find new configurations of turbine design. Next, instead of using the Jensen [17] or FLORIS model [18] to calculate wake effects, this study uses ECN FarmFlow, which showed a higher accuracy for large wind farms than other wake models in benchmark studies from 2009 to 2014 [19]. Finally, a recently developed technique for robust optimisation is used in this study.

This paper first outlines the optimisation method in section 2 followed by a description of the control variables, the objective function and the uncertainties in section 3. Section 4 describes the results from optimisation experiments and presents the main conclusions.

#### 2. Optimisation methodology

The methods for model-based optimisation for wind engineering objectives can be classified into derivative-based and derivative free techniques. This study considers a stochastic derivative based approach which has been shown to be effective for optimisation problems under uncertainty.

#### 2.1. Stochastic Simplex Approximate Gradient (StoSAG)

**1618** (2020) 042030

doi:10.1088/1742-6596/1618/4/042030

This paper considers an approximate (stochastic) gradient calculated with the StoSAG method developed by Fonseca et al. (2017) [20]. StoSAG is an approach which has shown to be powerful especially for optimisation problems which consider uncertainty and have a large number of control variables to be optimised. To approximate the gradient of the objective function with respect to control variables, an initial point is chosen (f.i. the point 0.25, 1 in Figure 1). Around this initial choice, the algorithm generates a set of normally (Gaussian) distributed perturbed controls, shown as blue dots in Figure 1. Once these points have been created the objective function values for each of these points will be evaluated, shown as the red dots. An approximate gradient is thereby calculated as a linear regression through this set of perturbed controls and corresponding objective function values. A standard gradient descent optimiser is then used in an iterative loop for the optimisation.

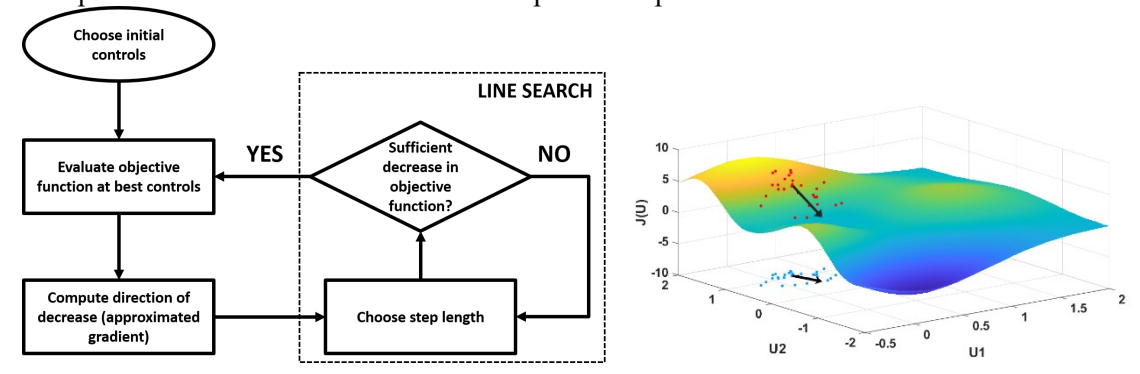


**Figure 1.** Schematic representation of the optimisation technique (left) and an example for a simple two control variable problem (right).

In a deterministic optimisation i.e. only a single model realisation of wind resource is considered, approximately ten perturbed controls (in this paper we use WFPD, RPD, Farm Orientation) are typically used to estimate the gradient. Therefore the ratio between model realisations and control variables is 1:10. In a robust optimisation experiment, with multiple model realisations to capture uncertainty (wind resource in this paper), the StoSAG method couples one model realisation (of the wind resource) with one perturbed control. Therefore the ratio between model realisations and perturbed controls is 1:1. With ten uncertain model realisations, this would mean the same computational effort as deterministic optimisation. The computational efficiency of the StoSAG method lies in its approach to estimate a robust gradient using a number of simulations equal to the number of model realisations. This is significant especially when evaluating high fidelity full physics simulation models, making it computationally attractive in large scale optimisation problems. For details into the theoretical aspects of the StoSAG technique we refer to [20].

### 3. Control variables, objective function, models & uncertainties

#### 3.1. Control Variables

In this paper, three control variables are optimised in various experiments. Adding more control variables to the optimisation problem is possible and is a user's prerogative.

3.1.1. Rotor Power Density (RPD) Instead of choosing from a fixed list of turbines available in the market, this study references a research turbine (AVATAR) with a fixed nominal power of 10 MW and rated wind speed [21]. The design of this turbine is changed by varying its rotor diameter, and its power and thrust curves are scaled accordingly until rated wind speed. Increasing the turbine diameter increases the power production between cut-in and cut-out wind speeds and reduces thrust coefficients. To capture this, the first control variable is the rotor power density (RPD in W/m²), defined as the ratio of turbine nominal power to the rotor swept area. Therefore,

$$RPD = (P_{turbine})/((\pi/4)d^2)$$
 (1)

**1618** (2020) 042030

doi:10.1088/1742-6596/1618/4/042030

where d is the rotor diameter and  $P_{turbine}$  is the turbine nominal power.

3.1.2. Wind Farm Power Density (WFPD) In this study, the aim is to find the optimal number of turbines in a fixed farm area (equal to 150 km², with a defined length and width of 15 km and 10 km). A second control variable defined is wind farm power density (WFPD in MW/km²), which is the ratio of wind farm nominal power to farm area. The layout of the turbines is in a parallelogram shaped structure with as many "boundary" turbines as possible (while respecting the minimum spacing between turbines) and the remaining "centre" turbines equally placed in a grid within the boundaries. For each value of WFPD, a layout is generated such that the turbines are spaced fairly optimally in the attempt to reduce farm wake losses, due to which optimising the position of individual turbines is expected to provide only limited gain. Therefore,

$$WFPD = (P_{turbine} * n_{turbines}) / A_{farm}$$
 (2)

where  $n_{turbines}$  is the number of turbines in the farm and  $P_{turbine}$  is the turbine nominal power.

3.1.3. Farm Orientation ( $\theta$ ): WFPD only defines the layout and number of turbines in the farm. A third control variable, farm orientation angle ( $\theta$  in degrees) defines the direction towards which turbines in the farm are oriented. Farm orientation ( $\theta$ ) rotates turbines in the farm in the counter-clockwise direction (Figure 2).



**Figure 2.** Example wind farm layout with 76 turbines with  $\theta = 0^{\circ}$  (left) and  $10^{\circ}$  (right).

#### 3.2. Objective Function

The levelized cost of energy (LCoE) of a wind farm is the objective function and is defined as:

$$LCoE = ((Capex/a_n + Opex))/AEP$$
 (3)

where AEP (kWh/year), capex and annual opex are evaluated by the ECN wind cost model [22]. The annuity  $(a_n)$ , where r is average discount rate and n is the farm economic lifetime in years, is given by:

$$a_n = (1 - (1+r)^{-n})/r.$$
 (4)

Therefore, for each combination of WFPD, RPD and  $\theta$ , the evaluation of capex, opex and AEP results in a value of LCoE. The objective is to find the combination of RPD, WFPD and  $\theta$  that minimises LCoE.

$$LCoE_i = f(RPD_i, WFPD_i, \theta_i)$$
 (5)

For experiments which consider uncertainty, the objective function is the mean LCoE, which is calculated as the average over the LCoE for each model realisation. Other choices for objective functions like NPV or IRR can be considered, although these would be more powerful indicators with the inclusion of an energy market model that estimates the value of the electricity.

3.2.1. Capital expenses: Capex of a wind farm is modelled as a one-time investment, at the beginning of the project, and is calculated using different simulation models that compute costs for the wind turbine, support structure, electrical infrastructure and farm installation. Costs for wind turbine system including blades, hub, shaft, gearbox, generator, nacelle and electronic components are obtained from

**1618** (2020) 042030

doi:10.1088/1742-6596/1618/4/042030

engineering equations which assume scaling parameters that have been verified against many commercial turbines, as part of the offshore wind energy costs and potential (OWECOP) model [23]. For instance, the blade mass equation is expressed in terms of rotor power density and turbine diameter with some correction and scaling factors [24]. Support structure costs are determined by calculating the costs of tower, transition piece and monopile for a turbine, using TNO's UpWind monopile model [25]. A constant water depth for all individual turbine locations is assumed.

The electrical infrastructure model covers costs and electrical losses of the wind farm internal collection grid and the offshore transmission system up to the onshore grid connection point. ECN's EeFarm II tool [26] is used, which consists of a component database from which electrical components are chosen and parameterised based on the wind farm size, layout and location.

The installation model provides estimates for the cost of transport, installation and commissioning of wind farm components. ECN Install [27] provides these outputs based on the process steps that include rock dumping for scour protection, installation of monopiles, laying of intra array and export cables, installation of offshore high voltage substations, nacelles, blades & towers.

- 3.2.2. Operational expenses: ECN O&M Calculator [28] an operation and maintenance (O&M) software, provides estimates for the yearly operating costs. O&M is performed either by crew transfer vessels (CTV) or by service operation vessels (SOV). One CTV is assumed to maintain up to 60 wind turbines and one SOV up to 120 wind turbines. The number of technicians for corrective and calendar-based maintenance is estimated as a function of the number of wind turbines. The cost of spare parts scales with wind turbine size. To choose between CTVs or SOVs, an internal optimisation loop identifies the cheapest O&M strategy, by trying various combinations of vessels. The computational effort of the O&M module in relation to the other models used in the LCoE estimation, is relatively small.
- 3.2.3. Annual Energy Production: ECN FarmFlow calculates the wind turbine wake effects in (large) offshore wind farms by calculating the average velocities and turbulence intensities inside a wind farm. The wake model is a 3D parabolised Navier-Stokes code, using a k- $\varepsilon$  turbulence model to account for turbulent processes in the wake. The computational effort of ECN FarmFlow and the accuracy of its results is directly proportional to the number of wind speeds and wind directions chosen for evaluation. Compared to engineering models, due to its lengthy computation time of several hours to perform simulations across all wind speeds (at intervals of 1 m/s from cut-in to cut-out) and wind directions (at intervals of 5 degrees), an approximation method of ECN FarmFlow uses axial induction factor  $(a_x)$  to calculate the AEP. Axial induction factor  $(a_x)$  is calculated using the relation below, where  $C_T$  is the thrust coefficient.

$$C_T = 4a_r(1 - a_r) \tag{6}$$

In the approximation method, a single reference wind speed estimation of ECN FarmFlow (at 8 m/s) over all wind directions is simulated, and the resulting energy yield estimation is extrapolated over all wind speeds using the relation that axial induction factor at each wind speed  $(a_{vw})$  is proportional to the normalized difference between free stream and wake stream winds. First, according to Equation 6, the axial induction factor at the reference wind speed  $(a_{ref})$  is calculated using the thrust coefficient at the reference wind speed from the wind turbine thrust curve. Next, the axial induction factor  $(a_{vw})$  at all other wind speeds are calculated using the thrust curve of the wind turbine. Using the FarmFlow evaluation at the reference wind speed, the free and wake stream wind speeds  $u_{vref}$  and  $u_{wref}$  are used in Equation 7 to calculate wake stream wind speed  $(u_w)$  at each free stream wind speed  $(u_v)$ .

$$\frac{a_{vw}}{a_{ref}} \propto \frac{(u_v - u_w)/u_v}{(u_{vref} - u_{wref})/u_{vref}} \tag{7}$$

Finally, the wake stream wind speeds are used to calculate the power output and net energy yield of the turbines. The results from this approximation method is validated against a full FarmFlow simulation

**1618** (2020) 042030

doi:10.1088/1742-6596/1618/4/042030

for a 750 MW wind farm, and showed minimal differences in results. The full FarmFlow simulation showed a farm efficiency (ratio of energy yield with and without wake losses) of 96.8%, whereas the approximated method resulted in a farm efficiency of 96.3%.

## 3.3. Wind resource modelling & uncertainties

The location assumed for this study is at the Borssele Wind Farm Zone Site III, and the Weibull parameters for the omnidirectional wind speed and per directional section are determined based on the HARMONIE data at various heights [29]. The Weibull probability density function is given by:

$$p(U) = (k/a) \left(\frac{U}{a}\right)^{k-1} exp\left[-\left(\frac{U}{a}\right)^{k}\right]$$
 (8)

with shape parameter k and scale parameter a (in m/s) and for wind speed U.

From wind and energy rose plots (Figure 3) created using scale and shape parameters at 100 m from the HARMONIE data at Borssele Wind Farm Zone Site III [29], the main wind direction is seen to be from southwest.

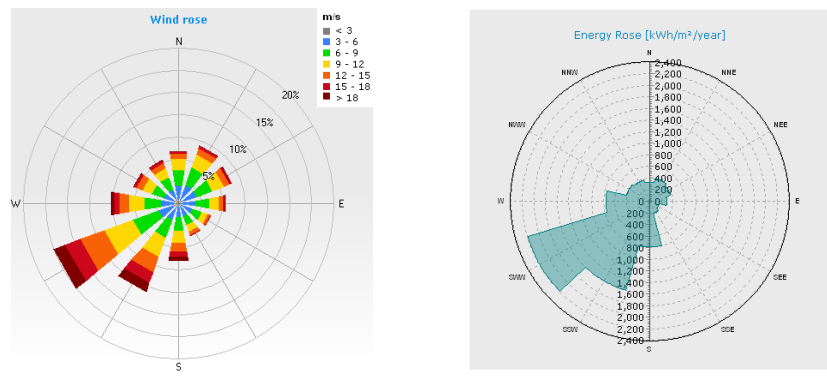
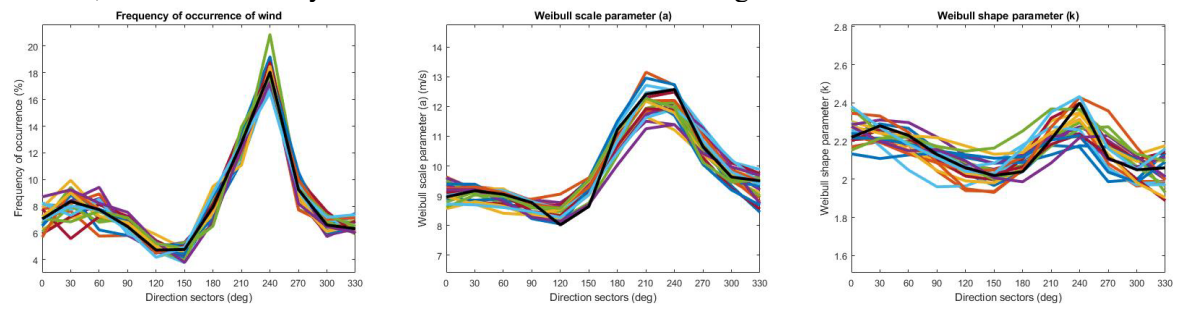


Figure 3. Wind and energy rose plots at the reference site (Borssele Wind Farm Zone Site III).

3.3.1. Uncertainty in wind resource: Using a Weibull distribution to represent the wind speed distribution, the uncertainty in wind resource can be expressed as uncertainty in the values of scale (a) and shape (k) parameters (see Equation 8). The scale parameter (k) is nearly proportional to the mean wind speed, and it is reasonable to assume that the percentage uncertainty in the mean wind speed is equal to the percentage uncertainty in k [14].

A 5% error, which is comparable to the values for three wind farms studied in [13] is assumed for the wind frequency as well as scale (k) and shape (a) parameters. This is done by generating twenty realisations of wind resources from a normal distribution with mean as true value of wind resource and error of 5%. The generated realisations are then fit with a smoothing spline curve line, with the black line showing the initial measured value of frequency, k and a. The generated values of the uncertain parameters, used in the twenty model realisations are shown in Figure 4.



**Figure 4.** Twenty realisations for uncertain parameters (frequency, scale parameter (a) and shape parameter (k)) with assumed uncertainty of 5%.

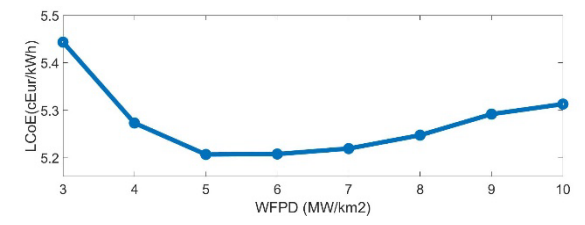
**1618** (2020) 042030

doi:10.1088/1742-6596/1618/4/042030

#### 4. Results

#### 4.1. Sensitivity analysis

Before the optimisation experiments, a sensitivity analysis is done, where the objective function is evaluated for different values of the control variables. Figure 5 shows the sensitivity of LCoE with varying WFPDs (at a constant RPD of 325 W/m<sup>2</sup> and a farm angle of 20°) and with varying RPDs (at a constant WFPD of 5 MW/km<sup>2</sup> and a farm angle of 20°).



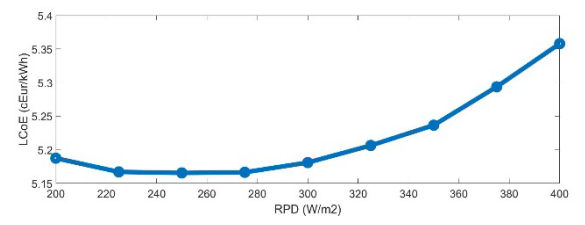


Figure 5. Sensitivity analysis of LCoE with varying WFPD (left) and RPD (right).

A minimum LCoE is seen at a WFPD of ~5 MW/km². The LCoE decreases until this value since the AEP continues to offset the capex and opex costs. Beyond this value, the LCoE increases since turbines are placed too close to each other resulting in wake losses and a failure of AEP to offset capex and opex costs.

Increasing RPD reduces rotor diameter, farm energy yield and farm capacity factor. An increase in RPD initially sees a lowering of LCoE since wake effects reduce and the decrease in energy yield is offset by the lower capex costs of turbines and support structures. However, beyond an RPD of  $\sim$ 250 W/m², the reduction in AEP and farm capacity factor is not offset by lower component costs.

Figure 6 shows the sensitivity of the LCoE to the farm orientation angle ( $\theta$ ). The most optimal orientation occurs around 140 degrees, where the shape of the farm is such that the least number of turbines are in the main wind direction (coming from southwest).

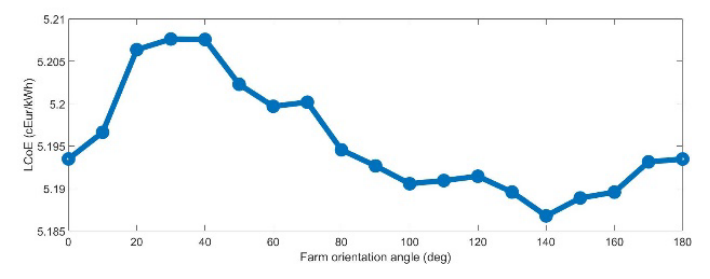


Figure 6. Sensitivity analysis of LCoE with varying farm orientation angle.

The sensitivity analysis results in a fairly optimal start point for the optimisation experiments. Any further reduction in LCoE would be a new improvement on the turbine and farm design. The optimisation experiments start with a simple problem with two control variables and no uncertainty (deterministic) and the complexity is increased with an addition control variable in farm angle and uncertainty in wind resource is later introduced. The reference LCoE for deterministic and robust start points are 5.144 c€/kWh and 5.152 c€/kWh respectively. The mean LCoE is higher in the robust case because of the twenty realisations that each define a wind direction frequency and scale and shape parameter and is a more robust representation of a future LCoE estimate of this wind farm.

**Table 1.** Initial turbine design, farm layout and LCoE of optimisation experiments.

Туре	Control variables	RPD (W/m²)	WFPD (MW/km²)	Farm angle (°)	Rotor diameter (m)	#turbines	LCoE (c€/kWh)
Deterministic, Robust	2, 3	250	5	140	225.7	75	5.144, 5.152

1618 (2020) 042030

doi:10.1088/1742-6596/1618/4/042030

### 4.2. Deterministic experiment results

Deterministic experiments with 2 control variables lower LCoE from 5.144 c€/kWh to 5.125 c€/kWh. Adding farm angle as a control variable further reduces the LCoE to 5.121 c€/kWh (0.45%). The optimised turbine diameter, farm layout and orientation are in Table 2.

**Table 2.** Optimised turbine design, farm layout and orientation of deterministic experiments.

Туре	Control variables		WFPD (MW/km <sup>2</sup> )		Rotor diameter (m)			% decrease in LCoE
Deterministic	: 2	265.5	5.178	140	219.0	78	5.125	0.37%
Deterministic	3	263.9	5.171	137.4	219.7	78	5.121	0.45%

The number of turbines in both cases is the same whereas there is a slight increase in rotor diameter. This is because when the farm angle is optimised (at 137.4°), the wake losses are lower and there is greater scope to slightly increase the rotor diameter and capture more wind from each turbine. Figure 7 shows the design space explored during the optimisation experiment.

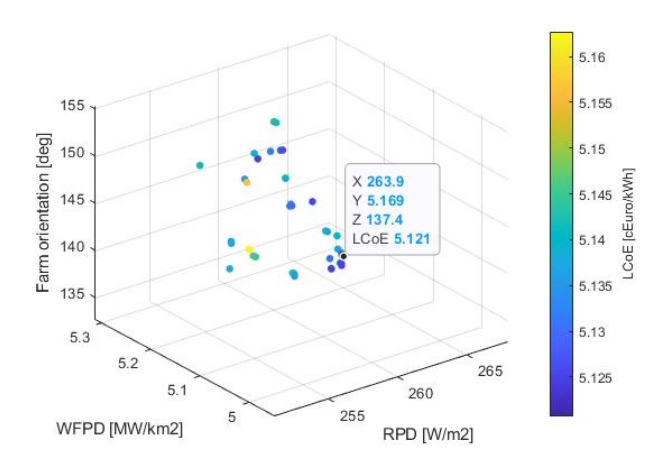


Figure 7. LCoE varying with WFPD (MW/km<sup>2</sup>) and RPD (W/m<sup>2</sup>) in an optimisation experiment.

# 4.3. Robust experiment results

Robust experiments assume an initial uncertainty of 5% in the frequency of wind direction and scale and shape parameters. With 2 control variables, the mean LCoE decreases from 5.152 c€/kWh to 5.129 c€/kWh. Adding farm angle as a control variable further reduces the mean LCoE to 5.128 c€/kWh (0.47%). The optimised turbine diameter, farm layout and orientation are in Table 3.

**Table 3.** Optimised turbine design, farm layout and orientation of robust experiments.

Type		RPD (W/m²)	WFPD (MW/km²)	Farm angle (°)	Rotor diameter (m)	#turbines	Mean LCoE (c€/kWh)	% decrease in mean LCoE
Robust	2	265.1	5.167	140	219.2	78	5.129	0.46%
Robust	3	264.1	5.169	131.9	219.6	78	5.128	0.47%

The optimised farm angle in the robust case is lower than in the deterministic case (131.9° compared to 137.4°). This is because the twenty realisations of wind resource cumulatively orient the main wind

**1618** (2020) 042030

doi:10.1088/1742-6596/1618/4/042030

direction slightly southwards. Another finding is that the rotor diameter and number of turbines in the farm do not change significantly with the inclusion of uncertainty in wind resource.

#### 4.4. Validation and discussion

To test the performance of the optimiser, the optimised points in the deterministic 3 variables case is run with a robust evaluation and vice versa. A robust evaluation of the deterministic optimised point results in a mean LCoE of 5.129 c€/kWh and a deterministic evaluation of the robust optimised point results in an LCoE of 5.122 c€/kWh, both of them being slightly higher than the optimised results in sections 4.2. and 4.3. This analysis, along with the results in Table 2 and Table 3 highlight the need for an optimiser to find non-trivial optimised turbine design, farm layout and orientation.

In future work, instead of LCoE, the net present value (NPV) of an offshore wind farm can be optimised for, by modelling various assets in an energy market model which can determine with a merit order, the future electricity price of a wind farm during operation.

Also, instead of assuming a fixed uncertainty, this value can be estimated from a historical metocean timeseries at the required wind farm site location. To estimate this uncertainty, the timeseries can be discretised to cluster sectors of wind directions per year. Then, a Weibull distribution can be fit within each discretisation to calculate the scale and shape parameters within each sector. A normal distribution can then be fit to the scale and shape parameters for each sector to calculate the standard error or uncertainty for each sector.

Other extensions could introduce farm length and width as control variables and allow the number and relative positions of turbines to change, resembling the WFLOP. Multi-objective optimisation of parameters independent from LCoE like LCA (life cycle assessment) can be added to the objective function.

#### 5. Conclusions

In this work, wind farm optimisation is performed to find the ideal design, number and orientation of turbines in a fixed-layout offshore wind farm, while considering uncertainty in wind resource. Optimised values of rotor diameter, farm layout and orientation are found which show an improvement of ~0.5% in LCoE compared to the most optimal solution found as a result of a sensitivity analysis. Starting from a different design would therefore lead to higher improvements in LCoE. Robust optimisation provides for the possibility to improve decision making by including uncertainty in wind resource, and finds optimised strategies that are different from those found by the deterministic optimisation. In the deterministic experiments, a slight increase in rotor diameter is seen when the farm orientation angle is optimised because the wake losses are lower and there is greater scope to change the rotor diameter and capture more wind from each turbine highlighting the non-trivial nature of the optimal solutions obtained in this work. In the robust experiments, an input uncertainty of 5% in the wind resource is reflected by twenty different wind realisations, resulting in overall decrease in LCoE of 0.47%. Various factors including the degree of uncertainty and nature of the objective function play a strong role in the results shown in this work. However we have shown that for almost the same computational effort uncertainty can be incorporated into the optimisation which might be very useful for many challenges in wind farm layout design.

# References

- [1] Walsh C, Ramirez R, Fraile D and Brindley G 2020 Offshore Wind in Europe: Key trends and statistics Wind Europe
- [2] Yang H, Chen J and Pang X 2018 Wind Turbine Optimization for Minimum Cost of Energy in LowWind Speed Areas Considering Blade Length and Hub Height *Appl. Sci.* **8** 1202
- [3] Biswas P, Sugunathan PN and Amaratunga G 2017 Optimization of Wind Turbine Rotor Diameters and Hub Heights in a Windfarm Using Differential Evolution Algorithm *Sixth*

**1618** (2020) 042030

doi:10.1088/1742-6596/1618/4/042030

- *International Conf. on Soft Computing for Problem Solving* Singapore Springer nature p. 131-141.
- [4] Stanley A, Thomas J, Annoni J, Dykes K, Fleming P and Ning A 2017 Gradient-Based Optimization of Wind Farms with Different Turbine Heights *American Institute of Aeronautics and Astronautics* Dallas National Renewable Energy Laboratory p. 1619.
- [5] Eminoglu U 2016 Site-specific design optimization of horizontal-axis wind turbine systems using PSO algorithm *Turkish Journal of Electrical Engineering & Computer Sciences* **24** 1044 1060
- [6] Feng J and Zhong Shen W 2015 Solving the wind farm layout optimization problem using random search algorithm *Journal of Renewable Energy* **78** 182-192
- [7] Feng J and Zhong Shen W 2017 Design optimization of offshore wind farms with multiple types of wind turbines *Applied Energy* **205** 1283-1297
- [8] Charhouni N, Sallaou M and Mansouri K 2019 Realistic wind farm design layout optimization with different wind turbines types *Int J Energy Environ Eng* **10** 307–318
- [9] Stanley A and Ning A 2019 Coupled wind turbine design and layout optimization with nonhomogeneous wind turbines *Wind Energ. Sci* **4** 99–114
- [10] Graf P, Dykes K, Scott G, Fields J, Lunacek M, Quick J, et al. 2016 Wind Farm Turbine Type and Placement Optimization *J. Phys.: Conf. Ser* **753**
- [11] Roscher B, Harzendorf F, Schelenz R and Jacobs G 2018 Reduced Levelized Cost of Energy through Optimization of Tower Height, Rotor Diameter And Wind Farm Layout *American Journal of Engineering Research* 7(4) 130-138
- [12] Quick J, Dykes K, Graf P and Zahle F 2016 Optimization Under Uncertainty of Site-Specific Turbine Configurations *Journal of Physics: Conference Series* **753**(6)
- [13] Richter P, Wolters J, Cakar R and Verhoeven-Moesek A 2018 *Uncertainty Quantification of Offshore Wind Farms Using Monte Carlo and Sparse Grid* Research Article Karlsruhe: Karlsruhe Institute of Technology, Steinbuch Centre for Computing
- [14] Lackner M, Rogers A and Manwell J 2014 Uncertainty Analysis in Wind Resource Assessment and Wind Energy Production Estimation *Aerospace Sciences Meeting and Exhibit* Reno American Institute of Aeronautics and Astronautics
- [15] Kwon SD 2009 Uncertainty analysis of wind energy potential assessment *Applied Energy* **87**(3) 856-865
- [16] Taylor M, Mackiewicz P, Brower M and Markus M 2007 An Analysis of Wind Resource Uncertainty in Energy Production Estimates New York:
- [17] Jensen NO; 1983.A note on wind generator interaction. Roskilde: Risø National Laboratory p. 16.
- [18] Gebraad P and Wingerde JW 2014 A Control-Oriented Dynamic Model for Wakes in Wind Plants *J. Phys.: Conf. Ser* **524**
- [19] Bot E 2015 FarmFlow validation against full scale wind farms Public Petten: ECN Wind Energy Report No: ECN-E--15-045
- [20] Fonseca R, Chen B, Jansen JD and Reynolds A 2016 A Stochastic Simplex Approximate Gradient (StoSAG) for optimization under uncertainty *Int. J. Numer. Meth. Engng* **109** 1756-76
- [21] Savenije F, Schepers JG and Ceyhan O 2015 AVATAR: Advanced aerodynamic tools for large rotors *American Institue of Aeronautics and Astronautics*
- [22] Bulder B, Bot E and Bedon G 2016 *Optimal wind farm power density analysis for future offshore wind farms* Public Petten: ECN Wind Energy Report No: ECN-E--18-025

**1618** (2020) 042030

doi:10.1088/1742-6596/1618/4/042030

- [23] Kooijman HJT and F H 2001 Application of an advanced cost model in the different design phases of an offshore wind turbine Public Petten, Netherlands: ECN Wind Energy Report No: ECN-RX--01-058
- [24] Bulder B, Hagg F, Bussel G and Zaaijer M 2021 *DOWEC concept study. Task 12: cost comparison of the selected concepts* ECN publication Petten: ECN Wind Energy Report No: ECN-C--01-080
- [25] de Vries W 2011 Support Structure Concepts for Deep Water Sites: Deliverable D4.2.8 (WP4: offshore foundations and support structures) Project Deliverable Delft: TU Delft Hydraulic Engineering
- [26] Pierik JTG, Axelsson U, Eriksson E and Salomonsson D 2009 *EeFarm II: Description, testing and application* Public Petten, the Netherlands: ECN Wind Energy Report No: ECN-E--09-051
- [27] Asgarpour M, Dewan A and Savenije R 2015 Innovative Offshore Wind Installation Concepts: Commercial Proof using ECN Install Public Petten: ECN Wind Energy Report No: ECN-E-14-028
- [28] Asgarpour M and van de Pieterman R 2014 *O&M Cost Reduction of Offshore wind farms A novel case study* Public Petten: ECN Wind Energy Report No: ECN-E--14-028
- [29] Riezebos HJ 2015 Site Studies Wind Farm Zone Borssele: Metocean study for the Borssele Wind Farm Zone Site III Public Utrecht: Deltares Report No: 1210467-000-HYE-001 0